27. We binned spectra over 46° of longitude (centered at CML 300°) for Fig. 1, B and C (and Fig. 2, A and B), but over only 16° for Fig. 2C. Profile d is centered at CML 310°, leading to lower mean mixing ratios in Fig. 2B as compared with Fig. 2C (profile d). See detailed map in Fig. 3.
28. S. Mau et al., Geophys. Res. Lett. 34, L22603 (2007).
29. M. A. Mischna, M. I. Richardson, R. J. Wilson, D. J. McCleese, J. Geophys. Res. 108, 5062 (2003).
30. F. Poulet et al., Nature 438, 623 (2005).
31. J. Bibring et al., Science 312, 400 (2006).
32. J. F. Mustard et al., Nature 454, 305 (2008).
33. H. Hiesinger, J. W. Head III, J. Geophys. Res. 109, E01004 (2004).
34. D. Baratoux et al., J. Geophys. Res. 112, E08S05 (2007).
35. M. H. Hecht et al., Eos 89, Fall Meeting Suppl., U14A-04 (abstr.) (2008).
36. S. P. Kounaves et al., Eos 89, Fall Meeting Suppl., U14A-05 (abstr.) (2008).
37. T. Encrenaz et al., Icarus 195, 547 (2008).
38. M. D. Max, S. M. Clifford, J. Geophys. Res. 105, 4165 (2000).
39. D. S. Kelley et al., Science 307, 1428 (2005).
40. C. Wille, L. Kutzbach, T. Sachs, D. Wagner, E.-M. Pfeiffer, Glob. Change Biol. 14, 1395 (2008).
41. T. C. Onstott et al., Geomicrobiol. J. 23, 369 (2006).
42. L.-H. Lin et al., Science 314, 479 (2006).
43. J.-P. Bibring et al., Science 312, 400 (2006).
44. J. F. Mustard et al., Nature 454, 305 (2008).
45. R. Greeley, J. E. Guest, U.S. Geol. Surv. Map I-1802-B (1987).
46. D. E. Smith et al., J. Geophys. Res. 106, 23689 (2001).
47. We thank T. C. Onstott and L. M. Pratt for helpful comments and two anonymous referees for their comments and suggestions. This work was supported by NASA [the Planetary Analysis Program (RTOP 344-32-07 to M.J.M), Astrobiology Institute (RTOP 344-53-51, to M.J.M), and Postdoctoral Program (G.L.V.)]

Isotopic Evidence for an Aerobic Nitrogen Cycle in the Latest Archean

Jessica Garvin,[1] Roger Buick,[1]* Ariel D. Anbar,[2,3] Gail L. Arnold,[2] Alan J. Kaufman[4]

The nitrogen cycle provides essential nutrients to the biosphere, but its antiquity in modern form is unclear. In a drill core though homogeneous organic-rich shale in the 2.5-billion-year-old Mount McRae Shale, Australia, nitrogen isotope values vary from +1.0 to +7.5 per mil (‰) and back to +2.5‰ over ~30 meters. These changes evidently record a transient departure from a largely anaerobic to an aerobic nitrogen cycle complete with nitrification and denitrification. Complementary molybdenum abundance and sulfur isotopic values suggest that nitrification occurred in response to a small increase in surface-ocean oxygenation. These data imply that nitrifying and denitrifying microbes had already evolved by the late Archean and were present before oxygen first began to accumulate in the atmosphere.

All living organisms require fixed nitrogen for the synthesis of vital biomolecules, such as proteins and nucleic acids. Under low-oxygen conditions, nitrogen-fixing organisms meet this need by reducing dinitrogen gas (N_2) to ammonium (NH_4^+), which is readily incorporated into organic matter. All other organisms rely upon the degradation of N_2 fixers through ammonification to fulfill their nitrogen requirements. Although the evolved NH_4^+ is stable under anoxic conditions, the presence of O_2 in the surface ocean promotes nitrification, the microbial oxidation of NH_4^+ to nitrite (NO_2^-) or nitrate (NO_3^-). These oxidized species are either assimilated by organisms or, under low-oxygen conditions, biologically reduced and ultimately released to the atmosphere. The latter process provides a conduit for loss of fixed N from the ocean and proceeds via denitrification, the stepwise reduction of NO_3^- or NO_2^- to NO, N_2O, and finally N_2, or by anammox, the coupling of NH_4^+ oxidation to NO_2^- reduction. Because

unique isotopic fractionations are imparted during many of these transformations, the nitrogen isotopic composition $\delta^{15}N$ (1) of organic matter preserved in ancient sediments provides information about the evolution of the N cycle. Here we report $\delta^{15}N$ and total nitrogen (TN) measurements, as well as $\delta^{13}C_{org}$ and total organic carbon (TOC) data, obtained at a resolution of approximately one data point per meter from ~100 m of continuous drill core through the ~2.5–billion-year-old Mount McRae Shale, Hamersley Group, Western Australia (2).

If the fixed N reservoir is a steady-state system, the $\delta^{15}N$ of fixed N input and output will be equal ($\delta^{15}N_{input} = \delta^{15}N_{output}$). The isotope effect ε (3) imparted during fixed N input is approximated by the difference in $\delta^{15}N$ between the atmospheric N_2 source and the fixed N product ($\varepsilon_{input} = \delta^{15}N_{dinitrogen} - \delta^{15}N_{input}$, where $\delta^{15}N_{dinitrogen} = 0‰$), whereas that of the fixed N output is approximated by the difference in $\delta^{15}N$ between the oceanic fixed N source and the N_2 product ($\varepsilon_{output} = \delta^{15}N_{fixed N} - \delta^{15}N_{output}$). Thus, the mean $\delta^{15}N$ of oceanic fixed N is roughly equal to the difference in ε between the output and input processes ($\delta^{15}N_{fixed N} = \varepsilon_{output} - \varepsilon_{input}$). In the modern ocean, N_2 fixation is the primary source of fixed N, and denitrification the primary sink. Although fractionation during N_2 fixation is minimal, with $\varepsilon_{N_2 fixation} = -3$ to +4‰ (4, 5), the isotope effect

of denitrification from both NO_3^- and NO_2^- is large, with $\varepsilon_{denitrification} = +20$ to +30‰ (4). This results in a residual NO_3^- pool substantially enriched in ^{15}N. Thus, the +5‰ mean isotopic value of modern deep-ocean NO_3^- is attributed to the fractionation imparted during denitrification. Furthermore, because fixed N upwelled to the surface ocean is completely consumed by primary producers under most conditions (6), the $\delta^{15}N$ value of organic matter in well-preserved ancient sediments should record the mean $\delta^{15}N$ of oceanic fixed N.

The organic-rich Mount McRae Shale was deposited at 2.5 billion years ago (Ga), shortly before the main rise in O_2 2.45 to 2.22 Ga (7). Its geological setting, the sampling procedure, and analytical methods are described in the Supporting Online Material. In the lower portion of the sampled section (Fig. 1), $\delta^{15}N$ values average around +2.5‰ with relatively little variation (+1.3 to +3.8‰). They rise from +1.0‰ at ~161 m to a peak of +7.5‰ at 139 m, then fall back to +2.5‰. The rise in $\delta^{15}N$ roughly correlates with an enrichment in TOC between 153 and 126 m, from 3 to 16 weight percent (wt %). Additionally, atomic C/N ratios increase from ~150 to ~65 from base to top. $\delta^{13}C_{org}$ values vary little below 150 m, consistently falling between –36 and –42‰. There is no $\delta^{13}C_{org}$ excursion corresponding to the $\delta^{15}N$ spike. Instead, $\delta^{13}C_{org}$ values rise from –42 to –34‰ above 134 m, corresponding to a decrease in $\delta^{15}N$ values.

Given the low metamorphic grade (prehnite-pumpellyite facies to < 300°C) of the Mount McRae Shale (8), preferential $^{14}NH_4^+$ loss during high-temperature devolatilization should not have greatly affected $\delta^{15}N$ preservation (9). The direct relation between TN and $\delta^{15}N$ (Fig. 1) further supports minimal metamorphic $\delta^{15}N$ alteration because $^{14}NH_4^+$ loss would produce the opposite relation. The relatively high C/N ratios are typical of Precambrian organic matter (10) and reflect preferential degradation of organic N during diagenesis. The C/N decrease upsection may result from increased adsorption of diagenetically produced NH_4^+ onto clay minerals or its substitution for K^+ in K-bearing minerals. If so, the lack of covariation between $\delta^{15}N$ values and C/N ratios implies that diagenetic $\delta^{15}N$ alteration was

[1]Department of Earth and Space Sciences and Astrobiology Program, University of Washington, Seattle, WA 98195–1310, USA. [2]School of Earth and Space Exploration, Arizona State University, Tempe, AZ 85287, USA. [3]Department of Chemistry and Biochemistry, Arizona State University, Tempe, AZ 85287, USA. [4]Department of Geology, University of Maryland, College Park, MD 20742, USA.

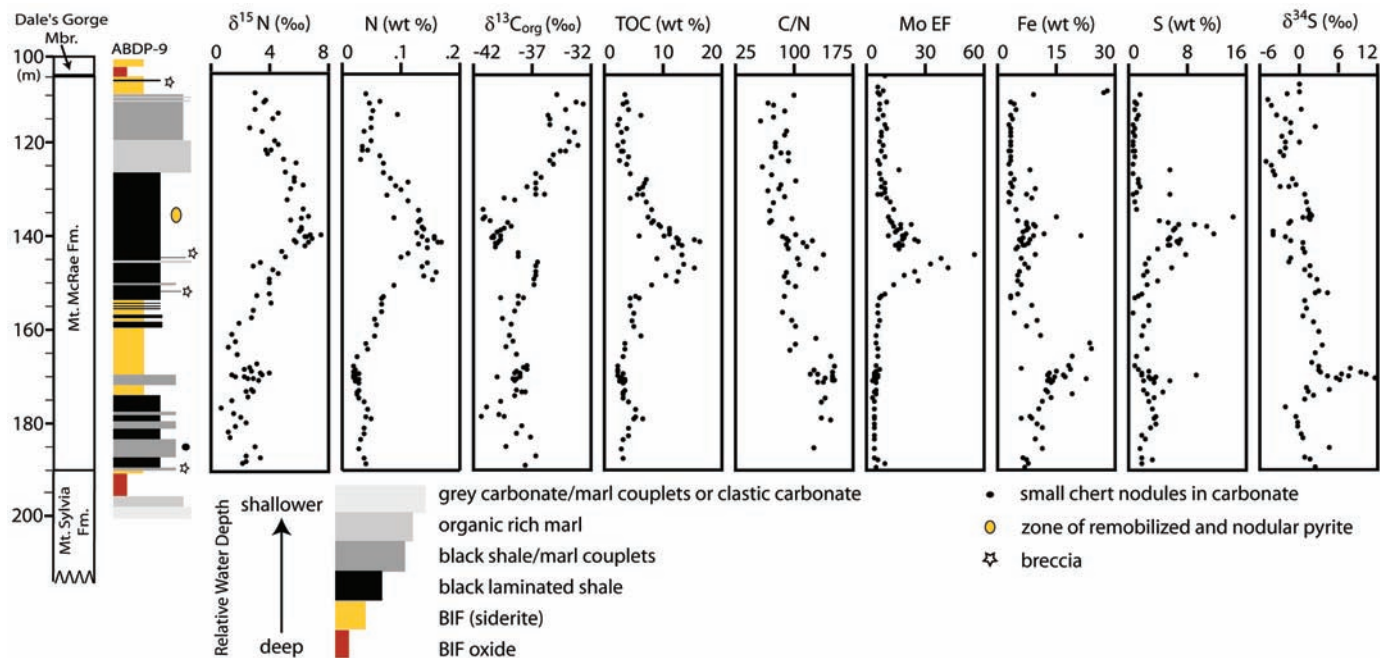*To whom correspondence should be addressed. E-mail: buick@ess.washington.edu
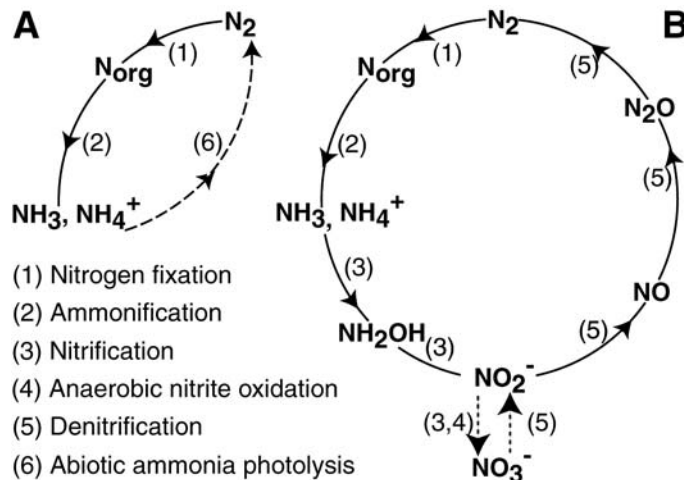
Fig. 1. Geochemistry of the Mount McRae stratigraphic section, including $\delta^{15}N$, TN, $\delta^{13}C_{org}$, TOC, atomic C/N, Fe and Mo enrichments, wt % S, and $\delta^{34}S$.

minimal. Furthermore, where bottom-water O_2 is low in the modern ocean, as it was during Mount McRae Shale deposition, there is little difference between the $\delta^{15}N$ of the original organic matter and that of diagenetically produced NH_4^+ (11). Thus, the $\delta^{15}N$ recorded in the Mount McRae kerogenous shales probably reflects the mean $\delta^{15}N$ of primary-producer biomass.

The $\delta^{15}N$ average of +2.5‰ below 161 m is less than the mean value of fixed N in the modern ocean (+5‰), indicating that little fractionation was imparted during fixed N input and output. This could reflect an environment similar to modern stratified basins where nitrification and denitrification are active and $\varepsilon_{denitrification}$ is under-expressed because NO_3^- is completely consumed at the oxic/anoxic interface (12). However, nitrification requires environmental O_2, but there is no evidence for its presence in this part of the core. In particular, the low amounts of sedimentary Mo below 161 m (despite high S and TOC contents, which should sequester any Mo if available) suggest that oxidative weathering of Mo-bearing sulfides in continental crust or detrital sediments was not active (13), precluding large amounts of atmospheric or oceanic O_2. Thus, it is more likely that the low $\delta^{15}N$ values below 161 m represent an anoxic N cycle with little fractionation imparted during microbial N_2 fixation and negligible fixed N loss (Fig. 2A).

The rise in $\delta^{15}N$ values to modern ocean values between 161 and 139 m indicates that fractionation occurred during fixed N loss. Although NH_3 loss to the atmosphere has an equilibrium isotope effect comparable to $\varepsilon_{denitrification}$ (14), this process should not have been favored because it is unlikely that Archean oceanic pH ever exceeded the limit (pH = 9.34) at which the NH_4^+-NH_3 equi-

Fig. 2. Nitrogen cycle transformations. (**A**) Hypothesized anaerobic N cycle before Mount McRae $\delta^{15}N$ excursion and (**B**) hypothesized suboxic aerobic N cycle at peak of Mount McRae $\delta^{15}N$ excursion. The broken line indicates abiotic processes, and the dotted line indicates plausible but unproven processes.

(1) Nitrogen fixation
(2) Ammonification
(3) Nitrification
(4) Anaerobic nitrite oxidation
(5) Denitrification
(6) Abiotic ammonia photolysis

librium shifts toward gaseous NH_3 (14, 15). Thus, increased expression of $\varepsilon_{denitrification}$ was evidently responsible for the increase in $\delta^{15}N$ values. The conversion of NO_3^- or NO_2^- to N_2 was probably biologically catalyzed because abiotic processes apparently reduce NO_3^- to NH_4^+ and not N_2 (16). Furthermore, expression of $\varepsilon_{denitrification}$ requires a large pool of NO_3^- or NO_2^- so that not all is consumed by denitrification. Thus, it is implausible that NO_2^- was a product of lightning combustion (17) because only a small amount of NO_2^- could have been produced by this process under late Archean conditions (18). Instead, it is most likely that microbial N_2 fixation introduced NH_4^+ to the ocean, and increased O_2 promoted the oxidation of NH_4^+ to NO_3^- or NO_2^-. Because high activation energy prevents NH_4^+ from abiotically oxidizing to NO_3^- or NO_2^- under Earth's surface

conditions, nitrifying microbes evidently produced the NO_3^- or NO_2^-. Microbial denitrification then imparted a N isotope fractionation to the residual oxidized N pool, recorded in organic N (Fig. 2B).

Correlative redox-sensitive trace metal (13) and S isotopic (19) data imply that intensification of nitrification and denitrification during the $\delta^{15}N$ excursion corresponded to a rise in O_2 from <10^{-6} to ≤10^{-5} present atmospheric level (PAL). Although increased oxygenation of the surface ocean may have limited N_2 fixation, and therefore productivity, during certain periods in Earth history (20), reduced N_2 fixation during the $\delta^{15}N$ excursion is unlikely. Although nitrogenase, the enzyme responsible for N_2 fixation, is irreversibly deactivated in the presence of molecular oxygen, inhibition is not apparent until the partial pressure of oxygen (P_{O_2}) > 0.2 to 0.5 PAL (21), which is
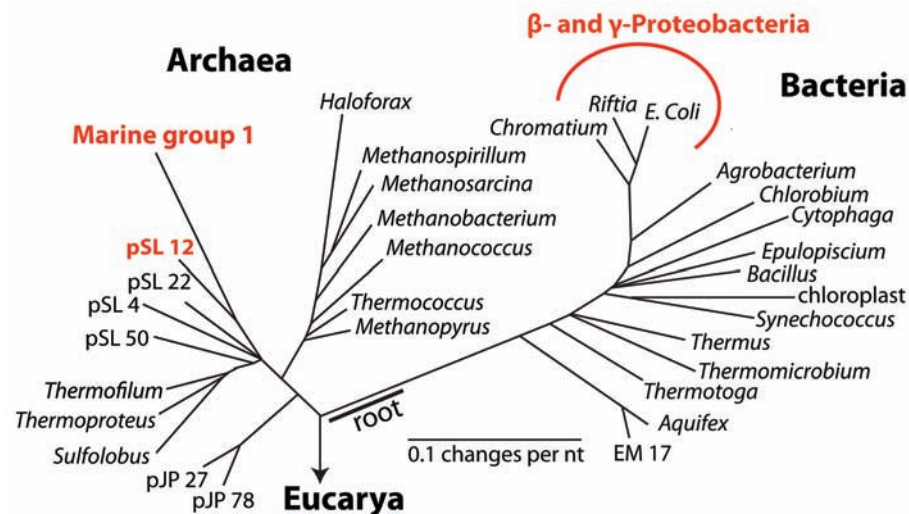
Fig. 3. The Tree of Life based on small subunit ribosomal RNA sequence analysis [modified from (29)]. Lineages in red represent known chemolithotrophic nitrifiers. The terminal position of Marine group 1 agrees with more recent widely accepted Archaeal trees [e.g., (30)].

much greater than the inferred maximum P_{O_2} of 10^{-5} PAL during the excursion. Furthermore, although Fe is a critical component of nitrogenase and the concentration of Fe^{2+} dropped during the $\delta^{15}N$ excursion (Fig. 1), cell culture experiments have shown that even under the low Fe concentrations characteristic of a fully oxygenated ocean, N_2 fixation rates are not lowered (22). Although NO_2^- may have been the most oxidized form of N attained under such low-oxygen conditions, incomplete nitrification would not have inhibited productivity because many microbes assimilate NO_2^- as effectively as NO_3^- (23). Thus, surface-ocean oxygenation during the $\delta^{15}N$ excursion was high enough to support nitrification, at least to NO_2^-, but not so high as to limit N_2 fixation, and therefore productivity.

The drop in $\delta^{15}N$ values above 139 m may indicate an increased proportion of sedimentary organic matter represented by N_2-fixing biomass. Alternatively, decreased $\delta^{15}N$ values may reflect decreased expression of $\epsilon_{denitrification}$. This could have resulted from diminished nitrification (because denitrification should approach complete consumption as the size of the NO_2^- or NO_3^- pool decreases), diminished denitrification, or both diminished nitrification and denitrification. Although the drop in $\delta^{15}N$ values is difficult to explain, decreased Mo and Fe abundances during this interval without a corresponding decrease in S concentrations (Fig. 1) indicate that the deep ocean may have become euxinic (anoxic and sulfidic). Because both nitrification and denitrification are deactivated under euxinic conditions (24), the formation of euxinic bottom waters—a plausible response to slight surface-ocean oxygenation and increased $[SO_4^{2-}]$ during the $\delta^{15}N$ excursion (20)—may have caused the observed drop in $\delta^{15}N$ values.

We conclude that the 2.5-Ga Mount McRae section records an episode of increased nitrification and denitrification in response to slight surface-ocean oxygenation. Thus, an aerobic component to the N cycle was transiently active before the atmosphere became oxygen-rich after 2.45 Ga (7). Previously, Beaumont and Robert (10) observed a range of kerogen $\delta^{15}N$ in cherts from –6.2 to +13‰ between 3.5 and 2.8 Ga, and +0.3 to +10.1‰ between 2.1 and 0.7 Ga, which they attributed to a transition from an anaerobic to an aerobic N cycle. More recent $\delta^{15}N$ data has complicated this scenario. For example, Jia and Kerrich (25) reported a trend from high $\delta^{15}N$ kerogen (+15.3‰) in highly metamorphosed Archean shales to low (+3.5‰) values in Proterozoic counterparts, whereas Shen et al. (26) noted that the largest positive $\delta^{15}N$ shift occurs in banded iron formations (BIFs) between 2.7 and 2.6 Ga, and not during the transition to a fully oxygenated atmosphere. These contradictory results illustrate the difficulty of interpreting $\delta^{15}N$ data from diverse samples with low stratigraphic resolution. For example, because Archean cherts are often associated with hydrothermal systems where chemolithoautotrophs ($\delta^{15}N_{biomass}$ = –9.6 to +0.9‰) replace photosynthesizers as the primary producers (26), the ^{15}N-depleted ancient cherts reported by Beaumont and Robert may reflect incorporation of chemosynthetic biomass, and not the mean $\delta^{15}N$ of oceanic fixed N.

Although denitrifying microbes are widespread across the Archaea and Bacteria, nitrification is more restricted phylogenetically (Fig. 3). The high productivity indicated by the high TOC and the attendant large positive nitrogen isotope fractionations suggests that nitrification could have been performed only by chemolithotrophic nitrifiers, because heterotrophic nitrifiers are, and presumably always were, minor contributors to the marine pool of oxidized nitrogen species. Because marine chemolithotrophic nitrifiers are apparently restricted to the β- and γ-Proteobacteria and the low-temperature marine group I.1 Crenarchaeota [although there are hints that pSL 12 Crenarchaeota might also nitrify (27)], and as these dominant nitrifying groups are terminally branching subphyla of peripheral clades of the Bacteria and Archaea (Fig. 3), our data imply that most prokaryotic phyla in at least one of these domains must have been extant by the time these groups arose. Thus, the macroevolution of microbes in the bacterial and/or archaeal domains may have been largely complete by the end of the Archean.

References and Notes

1. $\delta^{15}N(‰) = [(^{15}N/^{14}N_{sample} \div ^{15}N/^{14}N_{standard}) - 1] \times 1000$, where the $\delta^{15}N$ of the standard, represented by atmospheric N_2, is 0‰.
2. Geochronology constrains the age of the Mount McRae Shale to between 2501 ± 8 million years (1) and 2505 ± 5 million years (28).
3. $\epsilon(‰) = (^{14}\kappa/^{15}\kappa - 1) \times 1000$, where $^{14}\kappa$ and $^{15}\kappa$ are the rate coefficients of a reaction for the ^{14}N- and ^{15}N-containing reactants.
4. D. M. Sigman, K. L. Casciotti, in *Encyclopedia of Ocean Sciences*, J. H. Steele, K. K. Turekian, S. A. Thorpe, Eds. (Academic Press, London, 2001), pp. 1884–1894.
5. M. L. Fogel, L. A. Cifuentes, in *Organic Geochemistry*, M. H. Engel, S. A. Macko, Eds. (Plenum, New York, 1993), pp. 73–98.
6. M. A. Altabet, *Deep Sea Res. Part I Oceanogr. Res. Pap.* **35**, 535 (1988).
7. H. D. Holland, *Geochim. Cosmochim. Acta* **66**, 3811 (2002).
8. J. J. Brocks, R. Buick, G. A. Logan, R. E. Summons, *Geochim. Cosmochim. Acta* **67**, 4289 (2003).
9. G. E. Bebout, M. L. Fogel, *Geochim. Cosmochim. Acta* **56**, 2839 (1992).
10. V. Beaumont, F. Robert, *Precambrian Res.* **96**, 63 (1999).
11. M. A. Altabet et al., *Deep Sea Res. Part I Oceanogr. Res. Pap.* **46**, 655 (1999).
12. R. C. Thunell, D. M. Sigman, F. Muller-Karger, Y. Astor, R. Varela, *Global Biogeochem. Cycles* **18**, GB3001 (2004).
13. A. D. Anbar et al., *Science* **317**, 1903 (2007).
14. E. Wada, H. Hattori, *Nitrogen in the Sea: Forms, Abundances, and Rate Processes* (CRC Press, Boca Raton, FL, 1991).
15. D. L. Pinti, in *Lectures in Astrobiology*, M. Gargaud, B, Barbier, H. Martin, J. Reisse, Eds. (Springer, New York, 2005), vol. 1.
16. D. Summers, S. Chang, *Nature* **365**, 630 (1993).
17. Y. L. Yung, M. B. McElroy, *Science* **203**, 1002 (1979).
18. R. Navarro-Gonzalez, C. P. McKay, R. N. Mvondo, *Nature* **412**, 61 (2001).
19. A. J. Kaufman et al., *Science* **317**, 1900 (2007).
20. A. D. Anbar, A. H. Knoll, *Science* **297**, 1137 (2002).
21. I. Berman-Frank, Y.-B. Chen, Y. Gerchman, G. C. Dismukes, P. G. Falkowski, *Biogeosci. Discuss.* **2**, 261 (2005).
22. A. L. Zerkle, C. H. House, R. P. Cox, D. E. Canfield, *Geobiology* **4**, 285 (2006).
23. J. P. Zehr, B. B. Ward, *Appl. Environ. Microbiol.* **68**, 1015 (2002).
24. W. A. Kaplan, in *Nitrogen in the Marine Environment*, E. J. Carpenter, D. G. Capone, Eds. (Academic Press, New York, 1983), pp. 139–190.
25. Y. Jia, R. Kerrich, *Terra Nova* **16**, 102 (2004).
26. Y. Shen, D. L. Pinti, K. Hashizume, in *Archean Geodynamics and Environments*, K. Benn, J.-C. Maraschel, K. C. Condie Eds. (American Geophysical Union, Washington, DC, 2005), pp. 309–320.
27. T. J. Mincer et al., *Environ. Microbiol.* **9**, 1162 (2007).
28. B. Rasmussen, T. S. Blake, I. R. Fletcher, *Geology* **33**, 725 (2005).
29. N. R. Pace, *Science* **276**, 734 (1997).
30. C. Schleper, G. Jurgens, M. Jonuscheit, *Nat. Rev. Microbiol.* **3**, 479 (2005).

Zircon Dating of Oceanic Crustal Accretion

C. Johan Lissenberg,[1,2]*† Matthew Rioux,[3] Nobumichi Shimizu,[2]
Samuel A. Bowring,[3] Catherine Mével[1]

Most of Earth's present-day crust formed at mid-ocean ridges. High-precision uranium-lead dating of zircons in gabbros from the Vema Fracture Zone on the Mid-Atlantic Ridge reveals that the crust there grew in a highly regular pattern characterized by shallow melt delivery. Combined with results from previous dating studies, this finding suggests that two distinct modes of crustal accretion occur along slow-spreading ridges. Individual samples record a zircon date range of 90,000 to 235,000 years, which is interpreted to reflect the time scale of zircon crystallization in oceanic plutonic rocks.

Nearly two-thirds of Earth's crust is formed at mid-ocean ridges. Crustal growth is controlled by the transfer of melt from the mantle to the crust. There has been extensive research on the rates and volume of extrusive volcanism, but the time scales of melt delivery from the mantle and the resulting patterns of intrusive magmatism in these settings are not well known. This is largely because of the inaccessibility of lower crustal sections and the limited spatial resolution of indirect methods such as seismic imaging.

Recently, U-Pb geochronology of samples from exposed lower crustal sections has begun to constrain the timing of intrusive magmatism beneath mid-ocean ridge spreading centers. Previous studies, from Atlantis Bank on the Southwest Indian Ridge (1) and Atlantis Massif on the Mid-Atlantic Ridge (2), used ion microprobe U-Pb geochronology of zircon to date the crystallization of igneous rocks intruded into the lower crust in these areas. These studies have provided considerable new insight into the time scales of magmatism at mid-ocean ridges, presenting evidence for protracted lower crustal growth, but the relatively low precision of ion microprobe spot analyses [1.5 to 43%, 2σ (1)] and the complex tectonic histories of these areas limit our understanding of magmatic processes at typical slow-spreading ridge segments.

We report chemical abrasion–thermal ionization mass spectrometry [CA-TIMS (3)] U-Pb zircon dates from the Vema lithospheric section (VLS), located at 11°N on the Mid-Atlantic Ridge. The single-grain CA-TIMS dates have an uncertainty of 0.07 to 0.79% (2σ), which corresponds to an error of ~10,000 to 106,000 years, more than an order of magnitude more precise than published ion microprobe dates on similar-age oceanic gabbros.

The VLS is exposed along the transverse ridge of the Vema Fracture Zone, which rises to ~450 m below sea level, and comprises litho-

sphere that was uplifted ~10 to 11 million years ago (Ma) as a result of plate flexure (4), thus exposing a full section of mantle peridotites, lower crustal gabbros, and basaltic upper crust formed along the Mid-Atlantic Ridge (Fig. 1). The studied samples come from a narrow (6 km) section of the VLS centered around 42°42′W (Fig. 1), which formed at ~13 Ma according to plate motion models (5). The crustal section exposed along the VLS in the study area represents the northern end of an ancient ridge segment ~60 km in length [the EMAR segment of (4, 6)], and the section is thin [~2.2 km (7)] relative to the off-axis trace of the ancient segment center to the south (6). The crustal section, including the lower crust, is continuous, and is not composed of gabbro plutons intruding mantle peridotites, unlike the commonly inferred composition of slow-spreading segment ends (8). Gabbros exposed along the VLS in the study area commonly contain Fe-Ti oxides, indicating extensive differentiation.

We obtained U-Pb dates of 31 zircon grains and grain fragments separated from five gabbroic samples that were collected by submersible craft and by dredging along the VLS (7, 9) (see supporting online material for sample descriptions, analytical techniques, and data). Individual zircon dates range from 13.75 to 13.25 Ma (Fig. 2) and show a good correlation with sample location
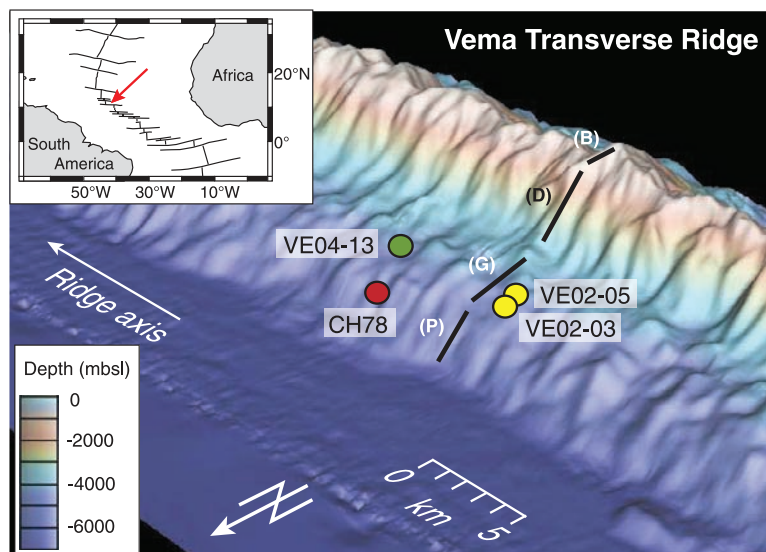
[1]Equipe de Géosciences Marines, Institut de Physique du Globe de Paris, 4 Place Jussieu, 75252 Paris Cedex 05, France. [2]Woods Hole Oceanographic Institution, Woods Hole, MA 02543, USA. [3]Department of Earth, Atmospheric, and Planetary Sciences, Massachusetts Institute of Technology, Cambridge, MA 02139, USA.

*Present address: School of Earth and Ocean Sciences, Cardiff University, Park Place, Cardiff CF10 3YE, UK.
†To whom correspondence should be addressed. E-mail: lissenbergcj@cardiff.ac.uk

Fig. 1. Location of samples dated in this study. Inset shows location of VLS within the Atlantic Ocean. Schematic geological section of the VLS (black solid lines) after (7). Samples with prefix VE were sampled by the submersible Nautile during the Vemanaute cruise (7, 9); samples with prefix CH were dredged during Jean Charcot Leg 78. On the basis of valley patterns observed in bathymetry, we estimate an along-axis uncertainty of 2 km for provenance of the dredged samples. P, peridotite; G, gabbro; D, dikes; B, basalt; mbsl, meters below sea level.